Ab-initio potential energy curves of valence and Rydberg electronic states of the PO radical

ARTICLE *in* COMPUTATIONAL AND THEORETICAL CHEMISTRY · DECEMBER 2014

Impact Factor: 1.55 · DOI: 10.1016/j.comptc.2014.10.001

5 AUTHORS, INCLUDING:

Najia Komiha

Mohammed V University of Rabat

53 PUBLICATIONS **278** CITATIONS

SEE PROFILE

Computational and Theoretical Chemistry 1049 (2014) 102–108

Contents lists available at ScienceDirect

Computational and Theoretical Chemistry

journal homepage: www.elsevier.com/locate/comptc

Ab-initio potential energy curves of valence and Rydberg electronic states of the PO radical

Safia Izzaouihda [a], Hassna Abou El Makarim [a], Najia Komiha [a,*], Souad Lahmar [b], Hassen Ghalila [b]

[a] LS3ME–Faculté des Sciences, Université Mohammed V Rabat Morocco, Morocco
[b] LSAMA–Faculté des Sciences, Tunis Al Manar, Tunisia

ARTICLE INFO

Article history:
Received 26 July 2014
Received in revised form 27 September 2014
Accepted 2 October 2014
Available online 12 October 2014

Keywords:
Electronic states
Spectroscopic constants
Highly correlated quantum chemistry methods
Potential energy curves
Spin-orbit couplings
Predissociation

ABSTRACT

This paper reports a theoretical study of the electronic states of PO radical. Highly correlated ab initio methods were used for mapping the potential energy curves. Internally contracted multi-reference configuration interaction method with the augmented correlation-consistent basis set (aV5Z) has been employed to carry out the study. After the nuclear motion treatment, the spectroscopic constants and the vibrational energy levels of the doublet and quartet electronic states are determined. The calculated values have been found in a good agreement with the existing experimental and theoretical results. The spin-orbit couplings between interacting states were also determined in the region where the crossings of the potential energy curves occurs. These couplings are capable to induce predissociation processes involving quartet states and producing P and O atoms at their ground and low lying excited electronic states. The theoretical vibrational spectrum was predicted using the Franck Condon factors and the transition moments integrals. The calculated spectrum shows intense peaks involving the Rydberg states in complete accordance with the experiment.

1. Introduction

PO, as CP and PN previously studied in our laboratory and by other authors, is a phosphorus containing molecule discovered in the interstellar medium, in the atmosphere of some planets, in cosmic dust or in carbon star envelops (IRC + 10216, Orion-KL, Sgr B2, W51A, TMC-1 [1,2]). Recently, PO has been detected by Tenenbaum et al. in Arizona Radio Observatory [3] in the envelope of an oxygen-rich supergiant star: VY Canis Majoris. All these phosphorus containing molecules can be concerned in the important oxygen, carbon, nitrogen–phosphorus chemistry supposed to exist in this medium [4–6]. The understanding of the P–O bond formation might also be of interest in biochemistry. Due to the importance of P–O bond, the PO molecule has also widely been studied experimentally. Chou et al. [7] synthesized nascent PO via collision free IR photolysis of dimethyl-methylphosphonate and studied the $B^2\Sigma^+ \rightarrow X^2\Pi$ transition. The same authors have studied the low lying excited states via Laser Induced Fluorescence after their formation in a microwave discharge. Seven valence electronic states and fourteen Rydberg states were experimentally identified by Coquart et al. [8] and, by mean of electron spin resonance (ESR), the values of a large number of spectroscopic constants [7,9] have been determined for the different electronic states.

The ab-initio studies concerning this radical and the related molecules have been published for decades [10–14]. Information about the lowest excited states, their vibrational levels, their photo-electronic spectra has been the subject of research since 1934 [15]. However, not much is known on the highly excited states, quartet states, long range potential energy curves of the Rydberg states and their spin-orbit couplings. In this work, the potential energy curves (PECs) of doublet, quartet and sextet states were calculated up to energies of 8 eV with accurate ab-initio quantum chemistry methods. Whereas most of the theoretical studies found in the literature only cover the equilibrium region of the valence states PECs, long range region were described here. In this work, the vibronic and spin-orbit couplings, the crossings of the PECs are determined in order to study the role of the quartet electronic states in the possible predissociation phenomena. Because of the high density of states and the somewhat complex angular momentum interactions, the analysis of the observed rotationally resolved spectra is quite difficult and accurate ab-initio calculations are definitely helpful to identify the involved electronic states.

* Corresponding author.
E-mail address: komiha@fsr.ac.ma (N. Komiha).

http://dx.doi.org/10.1016/j.comptc.2014.10.001
2210-271X/

2. Computational details

Calculations of the potential energy curves of the electronic states of PO were first performed using the SA-CASSCF [16] method with a quintuple zeta quality for the atomic orbital basis sets. These first CASSCF potentials serve to determine the most important electronic states and their dissociation limits. Following that, more accurate calculations, in order to obtain better results, were done: the highly correlated method MRCI (internally contracted multi-reference configuration interaction) associated to the large augmented correlation consistent polarised atomic orbital basis set (aug-cc-pV5Z, aV5Z) [17–19]. In order to describe properly the long range curves, the Davidson corrections were integrated to obtain the right dissociation limits. The av5Z basis sets for P and O atoms include diffuse orbitals in order to describe properly the upper electronic states. The calculations were performed in the C_{2v} symmetry subgroup. For the CASSCF calculations, 6 (four σ, one π_x and one π_y) molecular orbitals are included in the core [1–4σ, 1π] and two active spaces have been used. The first one is a full valence space (S1), including the [5–8σ, 2–3π] orbitals, sufficient to describe the valence states with all configurations obtained from excitations of the 11 valence electrons in the 8 (4 2 2 0 according to the symmetry) active orbitals. The second active space (S2) concerns the description of the Rydberg states. For that, it was necessary to add one more σ orbital in S2 [5–9σ, 2–3π]. This second active space was used to describe the $A^2\Sigma^+$ state since it is a 9sσ Rydberg state. The ground and $B^2\Sigma^+$ states were calculated in both active spaces as references for the excitation energies in the vibrational spectrum representation.

Concerning the CASSCF calculations of the Σ^+ doublet states, the number of configurations (CSFs) included in the reference space is 264 in the first active space and 1568 in the second active space. For the MRCI calculations, the references are then all configurations of the CI expansion of the CASSCF wave functions. For example, when computing the doublet states, more than 4.5×10^7 (6.5×10^5) non-contracted (contracted) configurations per C_{2v} symmetry are treated. These methods were used as implemented in the MOLPRO package [20] and are expected to yield a reliable description of the electronic states and good values for the spectroscopic parameters. Similar theoretical approaches have successfully been used in previous studies on PN and CP molecules [21] for an adequate description of all the electronic states.

Fig. 1 gives a global view of the potential energy curves (PECs) of all states calculated at the CASSCF/aV5Z level and shows highly excited bound electronic states. In the next step, MRCI calculations were performed and the nuclear motion problem was solved using distances around the minimum energy of the ground state. Standard perturbation calculations were performed using the Cooley and Numerov methods [22].

3. Results and discussions

3.1. The potential energy curves

The PECs of Fig. 1 correspond to the electronic states correlated to the four lowest dissociation asymptotes. Table 1 gives the calculated relative energies of these asymptotes as well as the corresponding NIST data [23]. They are found to be in a good agreement.

Fig. 1 shows a high density of electronic states, especially for energies >4 eV.

The PECs, calculated at the CASSCF/aV5Z level, are also depicted in Fig. 2a–d. For more clarity, potential curves of the states issued from the first, second, third and fourth asymptotes are shown separately.

Eleven states ($X^2\Pi$, $B^2\Sigma^+$, $B'^2\Pi$, $1^2\Phi$, $b^4\Sigma^-$, $C^2\Sigma^-$, $C'^2\Delta$, $F^2\Sigma^+$, $3^2\Pi$, $4^2\Pi$) were found bound. Their potential minima are for internuclear separations ranging from 2 to 5 bohr and are correlated to the two lowest asymptotes.

These valence excited states were calculated at the MRCI/aV5Z level (Fig. 3). In Fig. 4, the Rydberg states $A^2\Sigma^+$, $B^2\Sigma^+$ and the ground state $X^2\Pi$ are represented. The calculations are based on the S1 active space in the case of the valence states (Fig. 3) and S2 active space in the case of the Rydberg states (Fig. 4).

Using these PECs, the spectroscopic data were determined. Note that bound doublet and quartet electronic states exist also at high energies (up to 6 eV above the ground state minimum).

The electronic states calculated Table 3 are appointed in accordance to the notation of the theoretical and experimental studies of the literature [24,25]. The $X^2\Pi$ ground state and the lowest doublet excited state $B^2\Sigma^+$are correlated adiabatically to the first asymptote. The $B^2\Sigma^+$ state has been experimentally studied by Coquart et al. [8]. In complete agreement with this cited work, we find that this state is, at short distances, of Rydberg type with a semi diffuse character of the occupied $8\sigma^1$ orbital (see its electronic configuration in Table 2) and is only weakly bound (Table 3). This Rydberg state adiabatically correlates to the ground state asymptote because of the long range avoided crossing of the PECs of the same symmetry ($B^2\Sigma^+$–$F^2\Sigma^+$). The other experimentally

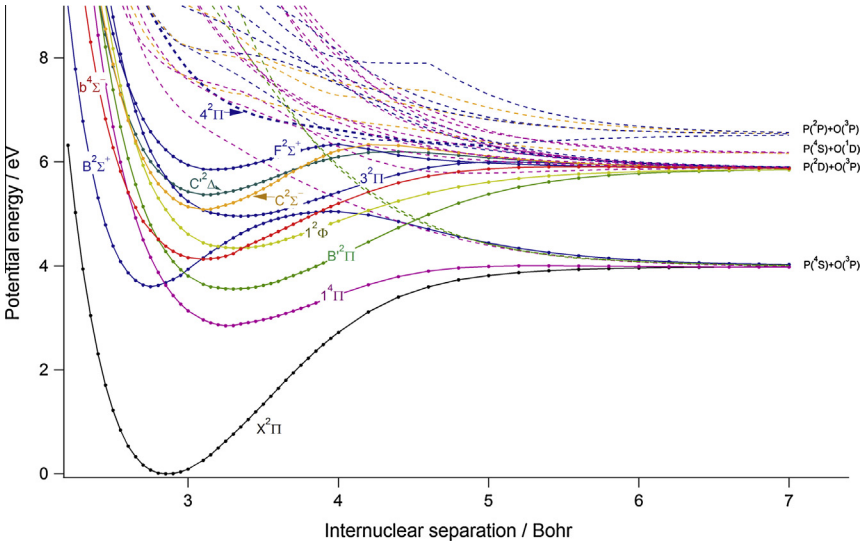

Fig. 1. Potential energy curves of the PO electronic states (CASSCF/aV5Z).

Table 1
Energies (eV) of the lowest dissociation asymptotes and correlated states.

	Ref. [23]	MRCI/av5z	Correlated states
$P(^4S) + O(^3P)$	0.0	0	$^{2,4,6}(\Pi, \Sigma^+)$
$P(^2D) + O(^3P)$	1.438663	1.50132	$^{2,4}(\Sigma^+, \Sigma^-, \Pi, \Delta, \Phi)$
$P(^4S) + O(^1D)$	1.967364	1.97232	$^4(\Delta, \Pi, \Sigma^-)$
$P(^2P) + O(^3P)$	2.352599	2.35927	$^2(\Sigma^+, \Sigma^-, \Pi, \Delta, \Phi, \Gamma)$

observed excited doublet states $B'^2\Pi$, $D^2\Pi$, $C^2\Sigma^-$, $C'^2\Delta$ and $D^2\Pi$ are correlated to the second asymptote. The $B^2\Sigma^+$ and $B'^2\Pi$ were found here to be very close in energy. The same can be said for the $C^2\Sigma^-$, $C'^2\Delta$ and $D^2\Pi$ states (see Table 3). The attribution of the electronic states can be considered as in overall agreement with available experimental and theoretical data [26,27].

The $A^2\Sigma^+$ Rydberg state, for which very few ab-initio calculations are available, has been properly described due to the use, in the CASSCF calculations, of a large active space including an additional σ orbital. The calculated spectroscopic numbers are in good agreement with the experiment (Table 4). A large number of mixed states and avoided crossings of the PECs of the same symmetry are shown. The existence of quartet states ($^4\Pi$ and $^4\Sigma^-$) whose corresponding PECs cross those of the low lying electronic states could induce predissociations toward the ground state asymptote through spin-orbit coupling. This has been predicted by Ngo et al. [28]. A great number of crossings between bound states curves can also induce vibronic couplings, favouring the dissociation of the excited states toward the lowest dissociation limit. The minima of the upper states curves have been described properly due to the use of large atomic orbital basis sets, including diffuse orbitals.

The main configurations of the different states calculated here are given in Table 2. Most of the states are multi-configurational and could be properly described by the accurate theoretical MRCI/aV5Z method used here.

3.2. Determination of the spectroscopic parameters of the different electronic states

The accurate PECs, needed for spectroscopic data determination, were used as potentials in the nuclear motion equations. The spectroscopic data and vibrational energy levels of the bound states were deduced.

The energies of the vibrational and rotational levels were obtained by solving the radial equation using the Numerov and Cooley methods [22]. The comparison with the experimental values has been made [24,25]. Tables 3 and 4 give the spectroscopic constants of the bound electronic states of PO including the equilibrium distances (bohr), the harmonic wavenumbers (cm^{-1}), the anharmonic term (ω_{ex}), the rotational constant (B_e), the dissociation and excitation energies (D_e and T_e).

The calculated values are in a good agreement with the experimental and previously published theoretical calculations [24,25]. For the ground state ($X^2\Pi$), our calculated equilibrium distance of 1.481 Å is in a good accordance with the experimental value of 1.476 Å given in reference [23]. A good agreement is also obtained for the harmonic wavenumber (ω_e), our value differs by less than 19 cm^{-1} from the experiment. For the other low electronic states, as shown in Table 3, the results are in reasonable agreement with the experimental values, with less than 0.02 Å error for the equilibrium distances, except for PO ($C'^2\Delta$) for which the deviation is

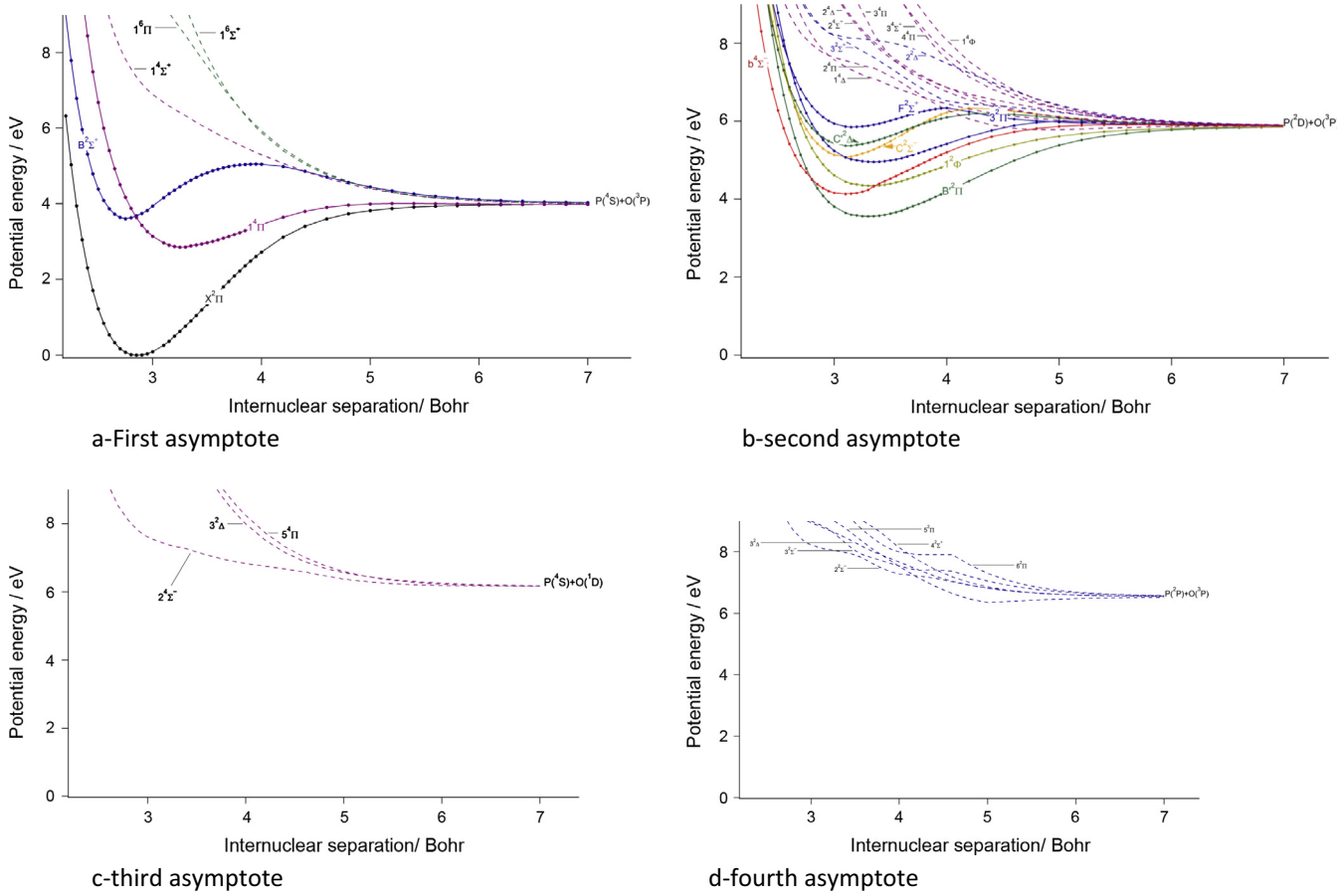

Fig. 2. Correlated states issued from the four lowest asymptotes (CASSCF/aV5Z).

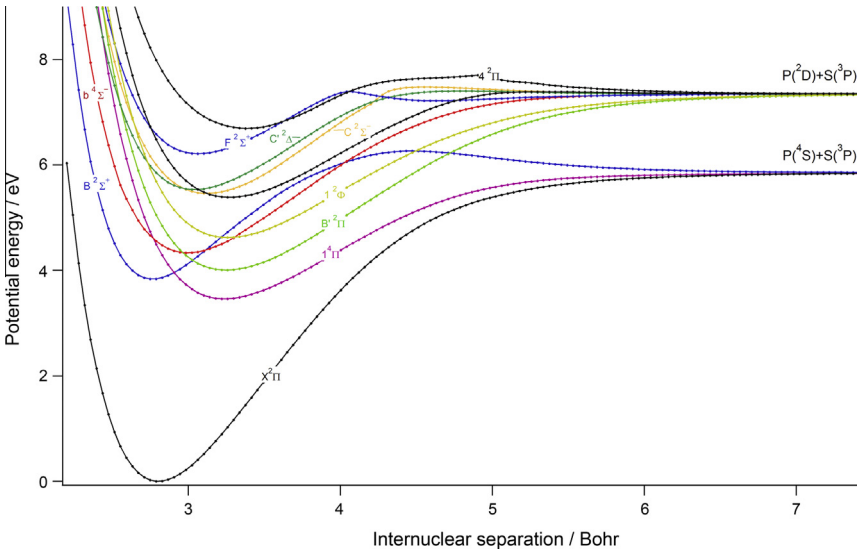

Fig. 3. MRCI potential energy curves of the electronic states of PO correlating to the two lowest dissociation limits (valence excited states).

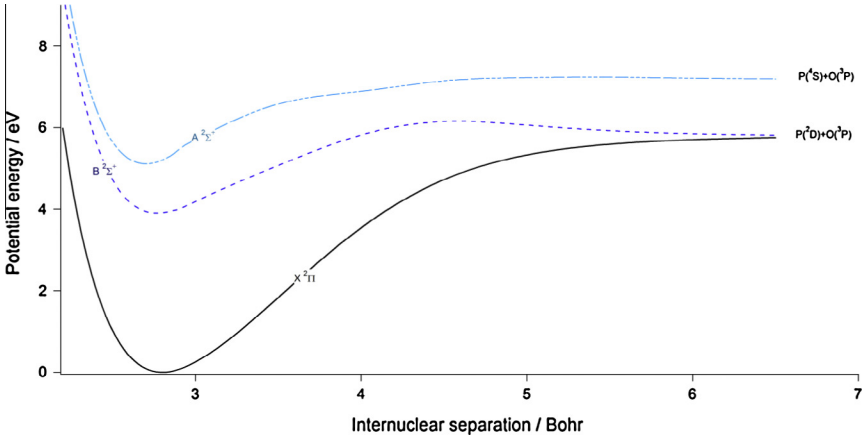

Fig. 4. MRCI/aV5Z potential energy curves of the Rydberg states $A^2\Sigma^+$, the $B^2\Sigma^+$ state and the ground state $X^2\Pi$.

around 0.2 Å. The harmonic wavenumber (ω_e) and the other spectroscopic constants are also close to the experimental values.

The spectroscopic data were particularly hard to calculate for the Rydberg states because of the numerous crossings of the PECs. Table 3 also shows the results for the quartet bound states. The only experimentally observed quartet state is the $b^4\Sigma^-$ [8]. Table 5 presents the vibrational energy levels for all those states. The calculated values of the vibrational energies agree with the experiment for the ground and first excited states [8,26–27,34–38]. It can be noticed that these vibrational levels are close in energy and this causes perturbations of the vibronic spectra [28]. Vibronic couplings may occur between these bound excited doublet states and the $1^4\pi$ state, leading to non-radiative transitions and to the dissociation of PO toward the lowest asymptote (Figs. 1–3).

3.3. Spin-orbit calculations

The calculations of spin-orbit coupling matrix elements between interacting states were carried out with an approach based on the Breit-Pauli operator as implemented in MOLPRO [20]. The previously described wave-functions obtained by the MRCI computations were used to set up the cartesian representation of the spin-orbit operator. The values of these couplings were calculated as a function of the interatomic distances. Strong spin-orbit interactions are shown at distances between 3 and 5 bohr. In this region, the rovibronic interactions are significant and the PECs of the different electronic states show crossings (Fig. 5). The couplings between doublet and quartet states exist through spin-orbit interactions and this favours predissociation processes.

One can conclude, for example, that the $A^2\Sigma^+$ is indirectly predissociated by the $1^4\pi$ state since the couplings between $A^2\Sigma^+$ and $B'^2\Pi$, $B'^2\Pi$ and $b^4\Sigma^-$, $b^4\Sigma^-$ and $1^4\pi$ are non-negligible. The indirect predissociation of the $A^2\Sigma^+$ state could also occur through the $3'^2\Pi$ and $B^2\Sigma^+$ states since the values of the spin-orbit couplings are significant. The direct predissociation of the $A^2\Sigma^+$ state towards the first dissociative asymptote and through the $1^4\pi$ is less favoured because of the weak values of the spin-orbit couplings (6.25–13.48 cm^{-1}).

The values of the spin-orbit couplings involving the quartet states show the important role of these states when studying the dissociation of the PO radical.

3.4. Simulated vibrational spectrum of PO

The theoretical vibrational spectrum is depicted in Fig. 6. We have provided the intensities distribution for the transitions

Table 2
Dominant configurations of the presently investigated electronic states of PO. These configurations are quoted for R_{P-O} = 2.8 bohr.

States	Electronic configurations	Coeff.
$X^2\Pi$	$(5\sigma)^2(6\sigma)^2(7\sigma)^2(2\pi)^4(3\pi)^1$	(0.94)
$1^4\Pi$	$(5\sigma)^2(6\sigma)^2(7\sigma)^1(8\sigma)^1(2\pi)^4(3\pi)^1$	(0.88)
$B^2\Sigma^+$	$(5\sigma)^2(6\sigma)^2(7\sigma)^2(8\sigma)^1(2\pi)^4$	(0.90)
$A^2\Sigma^+$	$(5\sigma)^2(6\sigma)^2(7\sigma)^2(8\sigma)^0(9\sigma)^1(2\pi)^4$	(0.90)
$b^4\Sigma^-$	$(5\sigma)^2(6\sigma)^2(7\sigma)^1(2\pi)^4(3\pi)^2$	(0.90)
$B'^2\Pi$	$(5\sigma)^2(6\sigma)^2(7\sigma)^2(2\pi)^3(3\pi)^2$	(0.60)
$1^2\Phi$	$(5\sigma)^2(6\sigma)^2(7\sigma)^2(2\pi)^3(3\pi)^2$	(0.50)
$C'^2\Delta$	$(5\sigma)^2(6\sigma)^2(7\sigma)^1(2\pi)^4(3\pi)^2$	(0.68)
$C^2\Sigma^-$	$(5\sigma)^2(6\sigma)^2(7\sigma)^1(2\pi)^4(3\pi)^2$	(0.77)
$3^2\Pi$	$(5\sigma)^2(6\sigma)^2(7\sigma)^2(2\pi)^3(3\pi)^2$	(0.84)
$F^2\Sigma^+$	$(5\sigma)^2(6\sigma)^2(7\sigma)^1(2\pi)^4(3\pi)^2$	(0.67)
$4^2\Pi$	$(5\sigma)^2(6\sigma)^2(7\sigma)^1(8\sigma)^1(2\pi)^4(3\pi)^1$	(0.45)

between the rovibrational levels of the $X^2\Pi$ state and those of the ($A^2\Sigma^+$, $B^2\Sigma^+$, $B'^2\Pi$, $C^2\Sigma^-$, $C'^2\Delta$, $F^2\Sigma^+$, $3^2\Pi$ and $4^2\Pi$) states of PO. For that, the Franck-Condon factors for all the transitions, involving rotational levels up to $N = 10$, were calculated using our MRCI potential energy curves and the LEVEL Program [39]. The transitions were fitted by Gaussian functions with a resolution (width at half maximum of the line) of 50 cm^{-1}. The line intensities were estimated from the Franck-Condon factors by adopting a Boltzman distribution to simulate the population of each rotational level at

Table 4
Spectroscopic constants of the ground and first Rydberg states ($A^2\Sigma^+$, $B^2\Sigma^+$) calculated at MRCI/aV5Z level with an extended active space for the CASSCF calculations (see text).

PO state	R_e/bohr	B_e/cm^{-1}	ω_e/cm^{-1}	$\omega_e x_e$/cm^{-1}	T_e/eV
$X^2\Pi$	2.8015	0.728	1216.3	10.97	0.00
Exp[a]	2.7902	0.734	1233.3	6.56	–
$B^2\Sigma$+	2.7694	0.744	1127.8	13.77	3.91
Exp[a]	2.7656	0.746	1164.5	13.46	3.81
$A^2\Sigma$+	2.7032	0.781	1329.8	36.00	5.21
Exp[a]	2.7051	0.780	1390.9	6.91	5.01

[a] Ref. [23].

Table 3
Spectroscopic constants of the valence excited electronic states.

	ω_e (cm^{-1})	ω_{ex} (cm^{-1})	B_e (cm^{-1})	R_e (bohr)	D_e (eV)	T_e (eV)
$X^2\Pi$						
This work	1214.60	6.69	0.727	2.7999	5.860	0
Exp [29]	1233.34	6.56	0.733	2.7902	5.474	
MRCI/aV6Z [30]	1232.89	6.56	0.729	2.7979	6.09	
$1^4\Pi$						
This work	770.9	8.82	0.545	3.2363	2.425	3.43
MRCI [31]	757.8	5.41	0.535	3.2660		3.38
$B^2\Sigma^+$						
This work	1174.2	13.90	0.747	2.7656	3.057	3.85
MRCI [31]	1152.3	10.95	0.738	2.7817		3.80
Exp [23]	1164.5	13.46	0.746	2.7663		3.81
$B'^2\Pi$						
This work	754.6	6.76	0.542	3.2463	5.257	4.01
MRCI [31]	764.2	4.77	0.537	3.2611		3.98
Exp [23]	759.2	3.85	0.542	3.2461		4.11
$b^4\Sigma^-$						
This work	881.4	7.07	0.635	2.9698	4.97	4.52
Exp [23]	889.0	6.62	0.644	2.9773		4.32
MRCI/aV6Z [30]	894.4	6.60	0.648	2.9660		4.26
$1^2\Phi$						
This work	733.1	5.23	0.537	3.2587	4.639	5.61
Exp [32]						
$D^2\Pi$						
This work	721.39	4.61	0.533	3.0397		6.41
$C^2\Sigma^-$						
This work	795.50	4.56	0.586	3.1229	3.785	5.81
Exp [33]	779.22	5.14	0.590	3.1248		5.56
MRCI/aV6Z [30]	797.12	5.11	0.589	3.1115		5.61
$C'^2\Delta$						
This work	836.5	6.85	0.618	3.0397	3.729	5.53
MRCI [31]	825.6	6.98	0.611	3.0575		5.70
Exp [23]	825.7	6.93	0.640	2.9868		5.42
$F^2\Sigma^+$						
This work	806.3	7.49	0.608	3.0643	3.057	6.21
Exp [32]	820	7.51	0.608	3.0642		6.18
$2^4\Sigma^-$						
This work	372.3	3.11	0.399	3.7802		6.28
$4^2\Pi$						
This work	692.4	2.52	0.496	3.2382		7.91

ω_e harmonic wave number .
ω_{ex} anharmonic wave number.
B_e rotational constant.
R_e equilibrium dis tance.
D_e dissociation energies.
T_e excitation energies.

Table 5
Vibrational energy levels (cm^{-1}) of the electronic states calculated from the different potentials.

V	$X^2\Pi$	$1^4\Pi$	$B^2\Sigma^+$	$A^2\Sigma^+$	$B'^2\Pi$	$b^4\Sigma^-$	$1^2\Phi$	$C'^2\Delta$	$C^2\Sigma^-$	$3^2\Pi$	$F^2\Sigma^+$	$4^2\Pi$
0	605.74	382.75	583.20	688.64	373.91	435.64	401.21	415.97	396.81	360.13	401.21	341.14
1	1806.89	1137.44	1729.33	2060.63	1114.52	1303.69	1192.64	1237.70	1184.57	1073.69	1192.64	1026.37
2	2994.59	1878.45	2846.85	3421.93	1847.73	2159.85	1969.49	2046.42	1967.14	1781.45	1969.49	1700.63
3	4168.76	2608.42	3935.24	4717.43	2577.61	3005.59	2732.02	2843.16	2747.15	2485.72	2732.02	2359.95
4	5329.36	3328.52	4993.99	5861.21	3304.02	3853.84	3480.62	3629.97	3526.46	3182.60	3480.62	3014.30
5	6476.32	4038.64	6022.66	6935.75	4023.03	4684.80	4215.72	4407.68	4302.52	3871.02	4215.72	3660.73
6	7609.63	4739.21	7020.92	7951.13	4735.98	5488.74	4940.08	5174.01	5070.59	4552.68	4940.08	4298.96
7	8729.30	5430.46	7988.64	8907.07	5442.46	6283.07	5655.30	5930.37	5830.86	5226.17	5655.30	4922.99
8	9835.36	6112.22	8926.00	9802.60	6142.23	7067.45	6355.74	6678.43	6582.60	5891.51	6355.74	5318.84
9	10927.79	6783.84	9833.83	10644.45	6834.92	7836.18	7040.89	7412.72	7323.84	6547.19	7040.89	5342.55
10	12006.57	7444.66	10714.29	11421.91	7520.00	8594.96	7709.17	8135.75	8057.15	7192.70	7709.17	–
11	13071.69	8094.43	11570.84	12133.98	8197.03	9336.66	8248.41	8846.19	8780.96	7827.47	8248.41	–
12	14123.12	8733.19	12405.18	12773.33	8865.99	10068.57	8356.22	9543.34	9495.78	8451.44	8356.22	–
13	15160.88	9360.76	13213.29	13332.86	9526.78	10787.19	8498.19	10226.72	10200.50	9064.40	8498.19	–

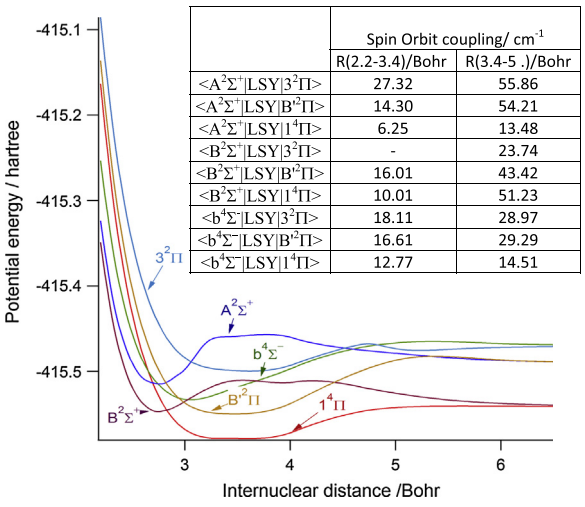

Fig. 5. Potentials and spin-orbit couplings between interacting states vs interatomic distances.

300 K. The spectrum is dominated, as expected, by the three most intense lines involving the Rydberg states: $X^2\Pi$–$B^2\Sigma^+$, $X^2\Pi$–$A^2\Sigma^+$ and $B^2\Pi$–$A^2\Sigma^+$. These three strong radiative transitions were clearly identified experimentally through Laser Induced Fluorescence (LIF) by Wong et al. [40]. Other less intense lines describing the transitions: $X^2\Pi$–$C^2\Sigma^-$, $X^2\Pi$–$C'^2\Delta$ and transitions between the $X^2\Pi$ and higher $^2\Pi$ and $^2\Sigma^+$states are also depicted in our theoretical spectrum. Those transitions have also been detected experimentally by several authors [28,33–36].

The quartet states, even not all observed, could be involved in possible non-radiative transitions and, through the spin orbit coupling, induce predissociation perturbations and energy transfer between states.

4. Conclusion and summary

This work shows that a large number of electronic states of the PO must be taken into account in explaining the spectroscopy of this radical. Many states are comparable in energy, with crossing PECs and mixed vibrational levels which may cause the interactions of different types: spin orbit, vibrational couplings, etc.

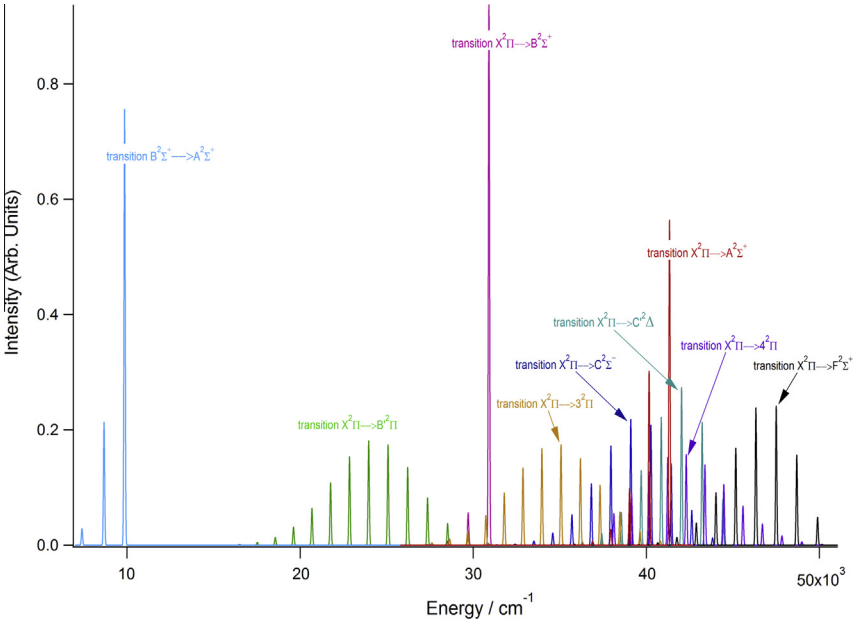

Fig. 6. simulated vibrational spectra of PO (transitions between ground state and valence doublet and Rydberg states).

The most important doublet and quartet states of PO have been accurately studied and the vibrational spectrum is effectively simulated. Evidence is also found showing that the calculated quartets are involved in non-radiative transitions and in predissociation processes due to the spin-orbit and vibronic couplings.

For this purpose, the potential energy curves have been determined using MRCI calculations associated with the large augmented correlation consistent basis set aV5Z. The long range PECs calculations have been performed so as to explain the dissociation processes.

The radial equation, giving the spectroscopic constants and the vibrational levels was solved using the Numerov and Cooley methods.

The spectroscopic data of the known states were found in good agreement with the experiment and previous theoretical work. The spin-orbit couplings have been estimated and show the interactions between states at short and long range.

The importance of the role of quartet states in the spectroscopy of PO radical has been pointed out.

The vibrational spectrum has been simulated showing that the three most efficient electronic transitions correspond to the experimentally detected systems involving the Rydberg states: $X^2\Pi$–$B^2\Sigma^+$, $X^2\Pi$–$A^2\Sigma^+$, $B^2\Sigma^+$–$A^2\Sigma^+$. Other transitions were found in the theoretical spectrum, two in agreement with the experiment: $X^2\Pi$–$C^2\Sigma^-$ and $X^2\Pi$–$C'^2\Delta$ [40] and the others involving higher $^2\Pi$ and $^2\Sigma^+$ states.

All this findings might be helpful for further research on the rather complicated spectroscopy of PO radical. The importance of the $A^2\Sigma^+$ Rydberg state as well as that of the $b^4\Sigma^-$ and $1^4\pi$ quartet states has been demonstrated and the accurate calculations performed here could properly describe all these states. This new findings are quite interesting since in the recent theoretical literature, the $A^2\Sigma^+$ state is not mentioned at all [41].

Acknowledgments

This work was carried out in the context of the projects Plan d'Urgence of the Ministry of Higher education of Morocco (SCH09/09), Tunisian-Moroccan MT07/12 and European PF7 Marie Curie PIRSES-GA-2012-317544 Project CapZeo.

References

[1] M. Guélin, J. Cernicharo, G. Paubert, B.E. Turner, Free CP In IRC+10216, Astron. Astrophys. 230 (1990) 9–11.
[2] S. Saito, S. Yamamoto, K. Kawaguchi, M. Ohishi, H. Suzuki, S.-I. Ishikawa, N. Kaifu, The microwave-spectrum of the CP radical and related astronomical, search, Astrophys. J. 341 (1989) 1114–1119.
[3] E.D. Tenenbaum, N.J. Woolf, L.M. Ziurys, Identification of phosphorus monoxide (X-2 Pi(r)) in VY Canis Majoris: detection of the first PO bond in space, Astrophys. J. 666 (2007) 29–32.
[4] W.M. Irvine, Organic-molecules in the gas-phase of dense interstellar clouds, Adv. Space Res. 15 (1994) 35–43.
[5] R.P. Wayne, Chemistry of Atmospheres, Clarendon Press, Oxford, 1991.
[6] A.R. Bossard, R. Kamga, F. Rawlin, Gas-phase synthesis of organophosphorus compounds and the atmosphere of the giant planets, Icarus 67 (1986) 305–324.
[7] J.S. Chou, D. Sumida, C. Wittig, Two-frequency two-photon ionization of nascent PO ($X^2\Pi$) from the collision-free IR photolysis of dimethyl methylphosphonate, Chem. Phys. Lett. 100 (5) (1983) 39–402.
[8] B. Coquart, M. Da Paz, J.C. Prudhomme, Spectre d'emission de la molecule PO: transitions $D^2\Pi$–$B^2\Sigma^+$ et $D'^2\Pi$–$B^2\Sigma^+$ des molécules $P^{16}O$ et $P^{18}O$. Reconsideration de l'etat de valence $D'^2\Pi$ Revue Canadienne de Physique 52(2) (1974) 177–183 (On the web since 2011).
[9] J. Kordis, K.A. Gingerich, Gaseous phosphorus compounds. IX. mass spectrometric studies of equilibria in the carbon–phosphorus system, J. Chem. Phys. 58 (1973) 5058–5064.
[10] C.M. Rohlfing, J. Amlof, Theoretical determination of the dipole-moment of carbon monophosphide, CP(X2-Sigma+), Chem. Phys. Lett. 147 (1988) 258–262.
[11] G. De Brouckère, Configuration interaction calculations of miscellaneous properties of the X(2)Pi(r) ground state, the C'(2) Delta excited state and related C'(2)Delta-X (2)Pi(r) transition bands of PO, J. Phys. B: At. Mol. Opt. Phys. (1999) 5283–5303.
[12] L.D. Knight Jr, J.T. Petty, S.T. Cobranchi, D. Feller, E.R. Davidson, The generation of C-12-P-31 and C-13-P-31 by reactive laser vaporization for rare-gas matrix electron-spin resonance studies – comparison with ab-initio theoretical calculations, J. Chem. Phys. 88 (1988) 3441–3450.
[13] P.E. Flemming, E.P.F. Lee, T.G. Wright, The ionization energy and Delta H-f (0 K) of CP, PCP and PCCP, Chem. Phys. Lett. 332 (2000) 199–207.
[14] B. Fernandez, P. Jorgensen, J. Simons, Calculation of hyperfine coupling-constants of the CN and CP ground-state radicals, J. Chem. Phys. 98 (9) (1993) 7012–7019.
[15] H. Von Barwald, G. Herzberg, L. Herzberg, Ann. Phys. 20 (1934) 38.
[16] P.J. Knowles, H.-J. Werner, An efficient second-order MC SCF method for long configuration expansions, Chem. Phys. Lett. 115 (1985) 259–263.
[17] H.-J. Werner, P.J. Knowles, An efficient internally contracted multiconfiguration reference configuration-interaction method, J. Chem. Phys. 89 (1988) 5803–5814.
[18] P.J. Knowles, H.-J. Werner, An efficient method for the evaluation of coupling-coefficients in configuration-interaction calculations, Chem. Phys. Lett. 145 (1988) 514–522.
[19] T.H. Dunning Jr., Gaussian-basis sets for use in correlated molecular calculations. 1. The atoms boron through neon and hydrogen, J. Chem. Phys. 90 (1989) 1007–1023.
[20] H.-J.Werner, P.J. Knowles, Molpro, a package of ab initio programs written, Version 2010 <http://www.molpro.net>.
[21] K. Abbiche, M. Salah, K. Marakchi, O.K. Kabbaj, N. Komiha, Ab initio study of PN electronic states – a qualitative interpretation of the perturbation and predissociation effects on observed transitions, Mol. Phys. 112 (1) (2014) 117–126;
K. Abbiche, K. Marakchi, N. Komiha, J.S. Francisco, R. Linguerri, M. Hochlaf, Accurate theoretical spectroscopy of the lowest electronic states of CP Radical Mol. Phys., 2014 (in press).
[22] J.W. Cooley, P.A.W. Lewis, P.D. Welch, The application of the fast Fourier transform algorithm to the estimation of spectra and cross-spectra, J. Sound Vib. 12 (3) (1970) 339–352.
[23] K.P. Huber, G. Herzberg, Molecular spectra and molecular structure, IV. Constants of Diatomic Molecules, Van Nostrand Reinhold, New York, 1979 <http://physics.nist.gov>.
[24] A. Metropoulos, A. Papakondilys, A. Mavridis, Ab initio investigation of the ground state properties of PO, PO+, and PO−, J. Chem. Phys. 119 (12) (2003) 5981–5987.
[25] G. De Broukère, Configuration interaction calculations of miscellaneous properties of the C '(2)Delta excited state and related C '(2)Delta-X-2 Pi(r) transition bands of phosphorus monoxide, Chem. Phys. 262 (2000) 211–2128.
[26] S.N. Gosh, R.D. Verma, A new valence $^2\Pi$ state of PO, J. Mol. Spectrosc. 73 (1979) 266–276.
[27] K.A. Peterson, R.C. Woods, An ab initio study of the 24 electron radicals PF, SO, NCl, SF+, ClO+, SiF−, PO−, NS−, and CCl− in their X3sigma- electronic states, J. Chem. Phys. 93 (1990) 1876–1888.
[28] T.A. Ngo, M. Da Paz, B. Coquart, C. Couet, Spectre d'émission de la molécule PO: Etude des états situés dans le domaine énergétique 50 000–58 000 cm^{-1} des molécules P16O et P18O, Rev. Canadienne de Phys. 52 (2) (1974) 154–158 (and references therein).
[29] T.V.R. Rao, R.R. Reddy, P.S. Rao, Potential energy curves and dissociation energy of the PO molecule, Physica C 106 (1981) 445–452.
[30] J.J. Sun, J.M. Wang, D.H. Shi, Multireference configuration interaction study on spectroscopic parameters and molecular constants of PO and PO+, Int. J. Quantum Chem. 112 (2012) 672–682.
[31] A. Spielfiedel, N. Handy, Potential energy curves for PO, calculated using DFT and MRCI methodology, Phys. Chem. Chem. Phys. 1 (1999) 2401–2409.
[32] S.N. Ghosh, R.D. Verma, Rydberg states of the PO molecule, J. Mol. Spectrosc. 72 (1978) 200–226.
[33] J.C. Prudhomme, M. Larzillière, C. Couet, Spectre d'émission de la molécule PO: transitions $C'^2\Delta$–$X^2\Pi$r et $C^2\Sigma$−–$X^2\Pi$r de $P^{16}O$ et $P^{18}O$, Can. J. Phys. 51 (2011) 2464–2471.
[34] M. Larzillière, M.E. Jacox, Infrared and ultraviolet absorption spectra of PO and HPO isolated in an argon matrix, J. Mol. Spectrosc. 79 (1980) 132–138.
[35] F. Grein, A. Kapur, Configuration interaction studies on low-lying valence and Rydberg states of PO, J. Chem. Phys. 78 (1982) 339–346.
[36] T.J. Tseng, F. Grein, Low-lying valence states of the PO molecule according to configuration-interaction calculations, J. Chem. Phys. 59 (1973) 6563–6571.
[37] S.P. Karna, P.J. Bruna, F. Grein, Configuration-interaction studies on the electronic states and structure of PS, J. Phys. B 21 (1988) 1303–1313.
[38] A.L. Roche, H. Lefebvre-Brion, Valence shell states of PO: an example of variation oft he spin-orbit coupling with internuclear distance, J. Chem. Phys. 59 (1973) 1914–1921.
[39] R.J. Le Roy, LEVEL 7.2, University of Waterloo Chemical Physics Research Report, CP-642, 2002.
[40] K.N. Wong, W.R. Anderson, A.J. Kotlar, Radiative processes following laser excitation of the A 2-Sigma+ state of PO, J. Chem. Phys. 85 (5) (1986) 2406–2413.
[41] H. Liu, D. Shi, J. Sun, Z. Zhu, Calculations on thirteen Λ-S states of PO radical: electronic structure, spectroscopy and spin-orbit coupling, J. Quant. Spectrosc. Radiat. Transfer 121 (2013) 9–22.